Relativistic Calculation of the Muonic Hydrogen Spectrum

J. D. Carroll* and A. W. Thomas
Centre for the Subatomic Structure of Matter (CSSM), Department of Physics, University of Adelaide, SA 5005, Australia

J. Rafelski
Departments of Physics and Mathematics, University of Arizona, Tucson, Arizona, 85721 USA

G. Miller
University of Washington, Seattle, WA 98195-1560 USA

(Dated: January 27, 2011)

The measurement of the $2P^{F=2}_{3/2}$ to $2S^{F=1}_{1/2}$ transition in muonic hydrogen and subsequent analysis has led to a conclusion that the rms radius of the proton differs from the accepted (CODATA) value by approximately 4%, leading to a 4.9σ discrepancy. We investigate the muonic hydrogen spectrum relevant to this transition using bound-state QED with Dirac wave-functions and comment on the extent to which the perturbation-theory analysis which leads to the above conclusion can be confirmed.

PACS numbers:

Contents

*Electronic address: jcarroll@physics.adelaide.edu.au

I. INTRODUCTION

The recent, extremely precise measurement of the measured transition energy between the $2P_{3/2}^{F=2}$ and $2S_{1/2}^{F=1}$ states of muonic hydrogen [1] has created considerable interest and speculation. The conclusion reached in that reference suggests that the value of the proton rms charge radius differs from that of CODATA [2] by 4.9 standard deviations. In an attempt to rectify this anomaly, avenues of research have included beyond standard model physics REF!, and claims of missing higher-order terms REF!. It is equally important however to be confident in the current analysis of the transition energy, which to this point has primarily involved perturbative calculations in QED [3–5].

In this work we calculate the transition energy relevant to the aforementioned experiment using the Dirac equation in an attempt to quantify the errors associated with the perturbative approach. In the sections following, we discuss the nature of the transition and its components, the method by which we calculate the energies corresponding to the various eigenstates, and summarise any discrepancies we find with respect to previous works.

II. MUONIC HYDROGEN SPECTRUM

The transition measured via laser spectroscopy of muonic hydrogen by Pohl *et al.* [1] at PSI involved detection of X-Rays corresponding to decays of a muon from the $2P_{3/2}^{F=2}$ state of muonic hydrogen to the $2S_{1/2}^{F=1}$ state, as depicted in Fig. 1.

The energy shift corresponding to this transition is complicated by the spectrum of muonic hydrogen in the following manner; the $2S_{1/2}$ eigenstate is shifted from the naïve energy of a muon residing in a point-Coulomb potential of magnitude

$$V_C(r) = -\frac{Z\alpha}{r}, \tag{1}$$

where Z denotes the number of protons, which for hydrogen $Z = 1$. Due to the fact that the proton charge-distribution is of finite-size (or rather the proton-form factor is not a delta-function), there is a shift from the naïve energy, denoted $\Delta E^{2S}_{\text{Finite}}$ in Fig. 1. The spin-orbit coupling of the muon to the proton leads to a hyperfine splitting of each of the eigenstates. For the case of the $2S_{1/2}$ eigenstate, this leads to hyperfine states with total angular momenta $F = 0$ and $F = 1$. The muon involved in the measured transition decays to the $2S_{1/2}^{F=1}$ state, and thus we require an accurate determination of the energy of this state and splitting. The 2S hyperfine splitting is denoted $\Delta E^{2S}_{\text{HFS}}$ in Fig. 1. The Lamb shift corresponds to the splitting of the $2S_{1/2}$ and $2P_{1/2}$ eigenstates due to vacuum polarization. These states are otherwise degenerate (as predicted by the Dirac equation). This splitting is denoted $\Delta E^{2S-2P}_{\text{Lamb}}$ in Fig. 1 and is the largest contribution to the measured transition by an order of magnitude. The splitting of the $2P_{1/2}$ and $2P_{3/2}$ eigenstates is predicted by the Dirac equation. Since the measured transition does not involve the $2P_{1/2}$ state, we shall only calculate the energy levels for the purpose of comparison to perturbative results. Both the $2P_{1/2}$ and $2P_{3/2}$ eigenstates are split by spin-orbit coupling into hyperfine states labelled by $F = 0$ and $F = 1$ for the $2P_{1/2}$ case, and $F = 1$ and $F = 2$ for the $2P_{3/2}$ case. The hyperfine splitting energies are denoted $\Delta E^{2P_{1/2}}_{HFS}$ and $\Delta E^{2P_{3/2}}_{HFS}$ for the corresponding states. The muon in the measured transition decays from the $2P_{3/2}^{F=2}$ eigenstate, so we require an accurate determination of the energy of this state.

III. NUMERICAL METHOD

To calculate the theoretical energy corresponding to the measured transition, previous authors have primarily used perturbation theory with non-relativisic wavefunctions to predict the size of the contributing effects, including relativistic corrections. In order to calculate the perturbative effect in the energy produced by a shift $V'(r)$ in the potential,

$$V(r) = -\frac{Z\alpha}{r} + V'(r), \tag{2}$$

we require a wave-function to integrate over. If we follow the methods of previous authors, we can use exact Schrödinger wave-functions for states with quantum numbers n, ℓ, m and perform the integration

$$\Delta E^{n\ell m}_{\text{V}'} \sim \int_0^\infty V'(r)\, |\phi^{n\ell m}_{\text{Schröd.}}(r)|^2 d^3r. \tag{3}$$

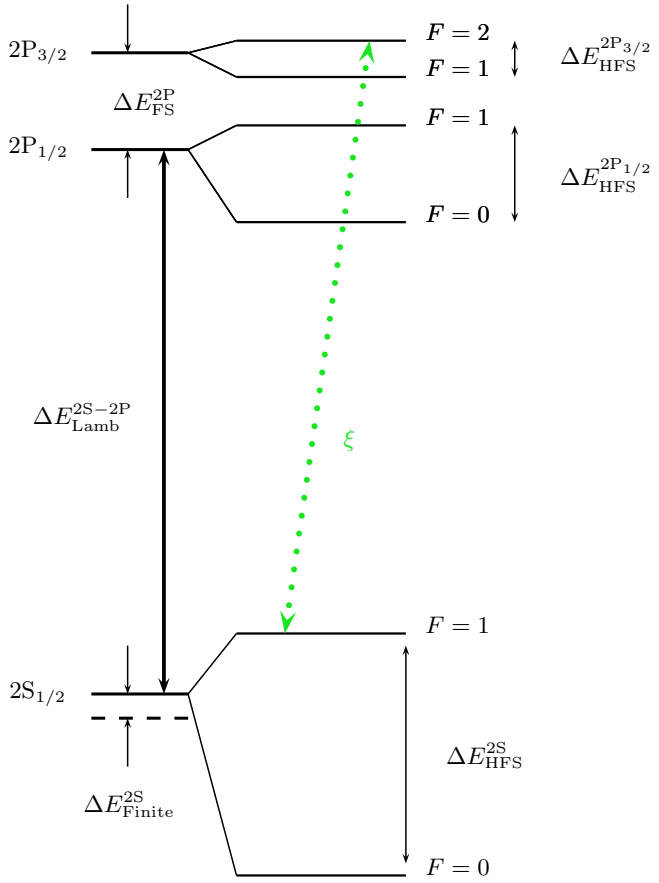

FIG. 1: (Color online) Muonic hydrogen spectrum, including finite-size correction, Lamb shift, fine structure, and hyperfine structure. Also shown is the measured $2S^{F=1}_{1/2}$ to $2P^{F=2}_{3/2}$ transition (green, dotted, ξ) as per Ref. [1].

To calculate the levels more precisely, we can use the Dirac Equation with the appropriate potential to calculate the perturbed wavefunctions. We consider the muon wavefunction in state α to be a spinor $\psi_\alpha(\vec{r})$

$$\psi_\alpha(\vec{r}) = \begin{pmatrix} g_\alpha(r)\chi^\mu_\kappa(\hat{r}) \\ -if_\alpha(r)\chi^\mu_{-\kappa}(\hat{r}) \end{pmatrix} = \begin{pmatrix} \dfrac{G_\alpha(r)}{r}\ \chi^\mu_\kappa(\hat{r}) \\ \dfrac{-iF_\alpha(r)}{r}\ \chi^\mu_{-\kappa}(\hat{r}) \end{pmatrix}, \tag{4}$$

normalised to unity, such that the probability is sensible

$$\int |\psi_\alpha|^2\, d^3r = \int_0^\infty r^2 \left[g_\alpha(r)^2 + f_\alpha(r)^2\right]\ dr = 1, \tag{5}$$

noting that

$$\int \chi^{m\dagger}_\kappa \chi^{m'}_{\kappa'}\ d\hat{r} = \delta_{\kappa\kappa'}\delta_{mm'}. \tag{6}$$

Since this is a relativistic system, we use the reduced mass μ in place of the muon mass in the Dirac Equation

$$\mu = \frac{M_p m_\mu}{M_p + m_\mu}. \tag{7}$$

Since the binding of the muon in this system is extremely weak, the eigenvalue ϵ_α for each state calculated using the Dirac equation is approximately equal to the reduced mass μ. In order to precisely calculate the variance from

this value, we shift our eigenvalue down by the reduced mass, such that the eigenvalue we are now solving for is $\lambda_\alpha = \epsilon_\alpha - \mu$. The Dirac equation we wish to solve is therefore given by

$$\frac{d}{dr}\begin{pmatrix} G_\alpha(r) \\ F_\alpha(r) \end{pmatrix} = \begin{pmatrix} -\dfrac{\kappa_\alpha}{r} & \lambda_\alpha + 2\mu - V(r) \\ -\lambda_\alpha + V(r) & \dfrac{\kappa_\alpha}{r} \end{pmatrix} \begin{pmatrix} G_\alpha(r) \\ F_\alpha(r) \end{pmatrix}, \tag{8}$$

where the value of κ_α is specific to each eigenstate, namely

$$\begin{aligned} 1\mathrm{S}_{1/2} : \kappa = \ -1, \quad 2\mathrm{S}_{1/2} : \kappa = \ -1, \\ 2\mathrm{P}_{1/2} : \kappa = \ +1, \quad 2\mathrm{P}_{3/2} : \kappa = \ -2. \end{aligned}$$

The (shifted) eigenvalues can be reliably reproduced by inserting the point-Coulomb potential of Eq. (1) into Eq. (8). In order to integrate Eq. (8), we supply an initial guess for the eigenvalue λ_α and appropriate boundary behaviour of upper and lower components of the wave-function at small and large radii, then integrate from each limit towards a central match-point. The normalised discontinuity in the wave-function integrated from each limit is used as a measure of the innacuracy of the eigenvalue and a refined estimate is calculated. This process is iterated until λ_α is less than the required tolerance, at which point we regard the wave-function to be converged.

IV. QUALITY CONTROL

To convince ourselves that our method is self-consistently accurate, We check the accuracy of our procedure using several methods. The unperturbed point-Coulomb Dirac eigenvalues are known analytically to be

$$\lambda_\alpha = \epsilon_\alpha - \mu = \mu \left[1 + \frac{Z^2\alpha^2}{(n_\alpha - |\kappa_\alpha| + \sqrt{\kappa_\alpha^2 - Z^2\alpha^2})^2} \right]^{-\frac{1}{2}} - \mu, \tag{9}$$

where n_α denotes the principle quantum number for state α. We first ensure that we are able to reproduce these values; for the $2\mathrm{S}_{1/2}$ wavefunction, we reproduce this value to within 0.01 μeV (we reproduce the $2\mathrm{P}_{1/2}$ eigenstate to within 40 neV, and the $1\mathrm{S}_{1/2}$ and $2\mathrm{P}_{3/2}$ eigenstates to within 10 peV) using quad-precision Fortran, a sufficiently large grid size, and sufficiently small grid spacing, within reasonable compute-time. We also check the validity of the virial theorem for our solutions (refer to Ref. [6] for further details) by calculating the reduced eigenvalue as

$$\lambda = \langle 2\mathrm{S}_{1/2} | \mu\beta + V(\vec{r}) + \vec{r} \cdot \vec{\nabla} V(\vec{r}) | 2\mathrm{S}_{1/2} \rangle - \mu, \tag{10}$$

which tests the accuracy of the muon wavefunction at the origin where $|\vec{\nabla} V|$ is greatest. We calculate that this term has a deviation from the value obtained using Eq. (9) of 0.18 μeV for a point-Coulomb potential, and 0.45 μeV the finite-Coulomb potential discussed in Sec. VI. We therefore conservatively take our errors to be of the order of $\sim \pm 0.5$ μeV. Propagating this error, we posess the ability to calculate the predicted proton rms charge-radius to within approximately 0.05 am (atto-metres, or 5×10^{-5} fm). We note that this calculation is therefore 12.8 times more precise than that of Ref. [1], itself 10.3 times more precise than that of Ref. [2]. This should be sufficient to examine the accuracy of the perturbative approach independently.

V. $2\mathrm{S}_{1/2}$–$2\mathrm{P}_{1/2}$ LAMB SHIFT

The Lamb shift is the splitting of the otherwise degenerate $2\mathrm{S}_{1/2}$ and $2\mathrm{P}_{1/2}$ eigenstates attributed to the vacuum polarization potential. We can calculate the effect that this has on the eigenvalues by assuming that this potential is a small perturbation of the Coulomb potential, and thus using Eq. (3) we find

$$\Delta E^{nlm}_{\mathrm{Lamb}} \sim \int_0^\infty V_{\mathrm{VP}}(r) \, |\Psi^{nlm}_{\mathrm{Schröd.}}(r)|^2 d^3r \,, \tag{11}$$

where V_{VP} is the vacuum polarization potential

$$V_{\mathrm{VP}}(r) = -\frac{Z\alpha}{r}\frac{\alpha}{3\pi}\int_4^\infty \frac{e^{-m_e q r}}{q^2} \sqrt{1 - \frac{4}{q^2}} \left(1 + \frac{2}{q^2}\right) d(q^2), \tag{12}$$

to which we must also add relativistic, recoil, and radiative corrections, as well as higher-order (in α) corrections.

Alternatively—and more accurately—we can calculate the shift in eigenvalues using converged Dirac wave-functions in response to the Coulomb and vacuum polarization potentials. In this case we simply take the difference between the converged eigenvalues for the $2S_{1/2}$ and $2P_{1/2}$ eigenstates calculated in the presence of a point vacuum polarization potential

$$\Delta E_{\rm Lamb}^{\rm 2S-2P} = \lambda_{\rm 2P_{1/2}} - \lambda_{\rm 2S_{1/2}}\,, \tag{13}$$

Care must be taken when comparing this calculation to that of Eq. (11) since our calculation includes relativistic corrections, which are calculated as corrections to Eq. (11) in Ref. [3]. A summary of this comparison, and the calculated values for the Lamb shift are given in Section IX.

VI. PROTON FINITE-SIZE CORRECTIONS

The perturbative leading-order contributions to the proton finite-size correction to the Lamb shift arise from considerations of the proton-form factor. These are derived in REF and appear in Ref. [1] as quoted from Ref. [3]. These terms are given by

$$\Delta E_{\rm Finite} = -\frac{2Z\alpha}{3}\left(\frac{Z\alpha\mu}{2}\right)^3\left[\langle r_p^2\rangle - \frac{Z\alpha\mu}{2}\langle r_p^3\rangle\right]. \tag{14}$$

To calculate this effect in our fully relativistic calculation, we consider the replacement of the point-Coulomb potential with the finite-size Coulomb potential in Eq. (8)

$$V_C(r) = -\frac{Z\alpha}{r} \to -Z\alpha\int\frac{\rho(r')}{|\vec{r}-\vec{r}'|}\,d^3r, \tag{15}$$

where $\rho(r)$ is the proton charge-distribution (or more accurately, the slope of the electric form-factor). We have studied the dependence of the finite-size correction on the form of this term (always normalised to unity) and this will be summarized in an upcoming publication (Ref. [7]), though the dependence on the choice of charge-distribution—whether it be exponential, Yukawa, or Gaussian in form—appears to be small.

The exponential form for the charge-distribution, normalised to unity such that $\int\rho(r)\,d^3r = 1$ is given by

$$\rho(r) = \frac{\eta}{8\pi}e^{-\eta r}; \quad \eta = \sqrt{12/r_p^2}\,. \tag{16}$$

We calculate the Lamb shift by taking the difference between the appropriate eigenvalues calculated using the Dirac equation with the potential given by Eq. (15) with the charge-distribution given by Eq. (16) for various values of r_p. We then interpolate the energy shifts and fit the data to a cubic of the form

$$f(x) = A\langle r_p^2\rangle + B\langle r_p^3\rangle, \tag{17}$$

which provides the relevant parameterization. The r_p dependence in the presence of an exponential finite-sized Coulomb potential and point vacuum polarization potential

$$V(r) = -Z\alpha\int\frac{\rho(r')}{|\vec{r}-\vec{r}'|}\,d^3r + V_{\rm VP}(r), \tag{18}$$

is given by

$$\Delta E_{\rm Finite} = -5.2000\langle r_p^2\rangle + 0.0350\langle r_p^3\rangle\ \text{meV}, \tag{19}$$

which is compared to the perturbative results in Section IX. Further to this contribution, we can consider the effect of convoluting the vacuum polarization (Eq. (12)) with the charge-distribution to investigate the finite vacuum polarization contribution. Thus,

$$V_{\rm VP}(r) \to -\frac{2Z\alpha^2}{3\pi}\int\frac{\rho(r')}{|\vec{r}-\vec{r}'|}Z_0(|\vec{r}-\vec{r}|)\,d\tau', \tag{20}$$

where we use the simplification given in Ref. [8] as

$$Z_n(|\vec{r}|) = \int_1^\infty e^{-\frac{2}{\lambda\!\!\!^{-}}|\vec{r}|\xi} \left(1 + \frac{1}{2\xi^2}\right) \frac{(1+\xi)^{\frac{1}{2}}}{\xi^n \xi^2} d\xi, \tag{21}$$

where $\lambda\!\!\!^{-}$ denotes the electron Compton wavelength (divided by 2π), $\lambda\!\!\!^{-} = 386.15926459$ fm. When discussing this potential, it should be assumed we are using the exponential charge-distribution. We once again calculate the eigenvalues using various values of r_p in the charge-distribution and fit the resulting energies to a cubic (as per Eq. (17)), except that in this case the vacuum polarization induces the Lamb shift, and we must include a term proportional to 1, thus we find

$$\Delta E_{\text{Finite}} = 205.182 - 5.2519\langle r_p^2\rangle + 0.0546\langle r_p^3\rangle \text{ meV}. \tag{22}$$

A summary of the calculations performed for this contribution and comparison to the perturbative values is given in Section IX.

VII. 2P FINE STRUCTURE

The $\mathcal{O}(Z\alpha)^4$ perturbative 2P fine structure shift is calculated in Ref. [4] to be

$$\Delta E_{FS}^{\text{2P}} = \frac{\mu^3 (Z\alpha)^4}{32 m_\mu^2} \left(1 + \frac{m_\mu}{2m_p}\right), \tag{23}$$

along with higher-order and other leading corrections. Taking this shift as the difference between the converged eigenvalues of the $2\text{P}_{1/2}$ and $2\text{P}_{3/2}$ eigenstates gives

$$\Delta E_{FS}^{\text{2P}} = \lambda_{2\text{P}_{3/2}} - \lambda_{2\text{P}_{1/2}}\,, \tag{24}$$

which we can also calculate in the presence of the various potentials. For the case of an exponential finite-Coulomb potential with finite vacuum polarization, the 2P fine structure shift is

$$\Delta E_{FS}^{\text{2P}} = 8.4206(5) \text{ meV}. \tag{25}$$

A comparison of this value with previous perturbative calculations is given in Section IX. The effect of the finite-size Coulomb potential (as compared to the point case) is below the level of errors for our calculation. Similarly, the effect of the finite-size vacuum polarization is also below our level of errors. The vacuum polarization itself increases the fine structure shift by 5 μeV.

VIII. HYPERFINE STRUCTURE

The hyperfine structure is a measure of the $\vec{\ell}\cdot\vec{\sigma}$ coupling. Following the lead of Ref. [9], the appropriate Hamiltonian is given by

$$\mathcal{H} = 2\beta\gamma\hbar \frac{\ell(\ell+1)}{j(j+1)} \left\langle \frac{1}{r^3} \right\rangle \mathbf{I}\cdot\mathbf{J} + \frac{16\pi}{3}\beta\gamma\hbar|\psi(0)|^2\, \mathbf{I}\cdot\mathbf{S}, \tag{26}$$

comprising a dipole term and a contact term, for which the following definitions apply for the muon Bohr magneton β_μ; proton Bohr magneton β_p; and proton gyromagnetic ratio γ

$$\beta_\mu = 2\alpha/m_\mu, \quad \beta_p = 2\alpha/M_p, \quad \gamma = 2(1+\kappa)\beta_p, \tag{27}$$

where $\kappa = 1.792847351$ is the proton anomalous magnetic moment. $\psi(0)$ represents the muon wavefunction at the centre of the proton. We investigate the two terms of Eq. (26) separately;

A. $2S_{1/2}$ Hyperfine Structure

There exist several methods by which the 2S hyperfine structure can be calculated. The perturbative 2S hyperfine structure calculated in Ref. [5] is given by

$$\Delta E_{HFS}^{2S_{1/2}} = \frac{1}{3}(Z\alpha)^4 \frac{\mu^3}{m_\mu m_p}(1+\kappa). \tag{28}$$

For $\ell = 0$ the contact term in the Hamiltonian (Eq. (26)) is non-zero, while the dipole term vanishes;

$$E_{HFS}^{2S} = \frac{16\pi}{3}\beta\gamma\hbar|\psi(0)|^2\langle Fm_F|\mathbf{I}\cdot\mathbf{S}|Fm_F\rangle\,, \tag{29}$$

where $|Fm_F\rangle$ is the eigenfunction belonging to $\mathbf{F} = \mathbf{I} + \mathbf{J}$, such that

$$\langle Fm_F|\mathbf{I}\cdot\mathbf{S}|Fm_F\rangle = \frac{1}{2}\left[F(F+1) - \frac{3}{2}\right]. \tag{30}$$

Thus, the splitting between the 2S $F = 0$ and $F = 1$ hyperfine levels is given by

$$\Delta E_{HFS}^{2S(F=1-F=0)} = \frac{16\pi}{3}\beta\gamma\hbar|\psi(0)|^2, \tag{31}$$

We note some important errors; in Ref. [4] Eqs. (27–28), the factors of 2 in the denominators of the third terms of should read 12. The calculations are performed correctly however. Furthermore, in Ref. [9] Eq. (18.2-17b), the sign should be positive and the second 9 in the denominator should not appear.

The value of the 2S hyperfine splitting, as calculated using Eq. (31) with the wavefunction calculated with the Dirac equation in the presence of the combined exponential finite-Coulomb and finite vacuum polarization potentials is

$$\Delta E_{HFS}^{2S} = 22.7690(5)\ \text{meV}. \tag{32}$$

We note that the effect of including the exponential finite-size Coulomb potential as compared to the point case reduces the splitting by 0.1269(5) meV; introducing the point vacuum polarization potential increases the splitting by 0.0747(5) meV for the point-Coulomb, and 0.0742(5) meV for the finite-Coulomb cases. Using the combined finite vacuum polarization and finite-Coulomb potentials reduces the splitting by 0.0012(5) meV to give the value above.

Alternatively, one can follow Ref. [**?**] in which case we can calculate this splitting to be

$$\Delta E_{HFS}^{2S} = \frac{\kappa g\mu}{\kappa^2 - \frac{1}{4}}\frac{\alpha}{2M_p}\left[\Lambda(\Lambda+1) - I(I+1) - j(j+1)\right]\int r^{-2}g(r)f(r)dr, \tag{33}$$

In that case, we calculate

$$\Delta E_{HFS}^{2S} = 22.7640(5)\ \text{meV}, \tag{34}$$

provided we correct for the reduced mass in the formula (note the error in Ref. [] in which this step is overlooked).

B. $2P_{1/2}$ Hyperfine Structure

The $2P_{1/2}$ Hyperfine structure is of no consequence to the measured transition we are investigating. Nonetheless, we calculate the energy of the $2P_{1/2}^{F=0}$ and $2P_{1/2}^{F=1}$ levels as a confirmation of our method, and to compare to the perturbative results. Following Ref. [4], to $\mathcal{O}(\alpha^4)$ the $2P_{1/2}$ hyperfine structure shift is given by

$$\Delta E_{HFS}^{2P_{1/2}} = E_F\left[\frac{1}{3} + \frac{a_\mu}{6} + \frac{m_\mu(1+2\kappa)}{12m_p(1+\kappa)}\right], \tag{35}$$

for which the Fermi energy is

$$E_F = \frac{\mu^3(1+\kappa)}{3m_\mu m_p}(Z\alpha)^4, \tag{36}$$

and where α_μ is the muon anomalous magnetic moment. Alternatively, for $\ell \neq 0$ the dipole term in the Hamiltonian (Eq. (26)) is non-zero, while the contact term vanishes. The energy for the dipole term is thus given by

$$E_{\rm HFS}^{2{\rm P}_{1/2}} = 2\beta\gamma\hbar\frac{\ell(\ell+1)}{j(j+1)}\left\langle\frac{1}{r^3}\right\rangle\langle Fm_F|\mathbf{I}\cdot\mathbf{J}|Fm_F\rangle, \tag{37}$$

where the non-zero terms in the dot-product are given by

$$\langle Fm_F|\mathbf{I}\cdot\mathbf{J}|Fm_F\rangle = \frac{1}{2}[F(F+1) - I(I+1) - j(j+1)]. \tag{38}$$

For Schrödinger wave-functions, the vacuum expectation value of r^{-3} is analytic, in that

$$\left\langle\frac{1}{r^3}\right\rangle = \left(a_0^3 n^3 \ell(\ell+1)(\ell+\frac{1}{2})\right)^{-1}. \tag{39}$$

Inserting the appropriate values of F, n, ℓ, I, j for each of the $F = 0$ and $F = 1$ states, one obtains the energy of the $2{\rm P}_{1/2}$ hyperfine structure to be

$$\Delta E_{\rm HFS}^{2{\rm P}_{1/2}} = \frac{2}{9}\beta\gamma\hbar/a_0^3. \tag{40}$$

Eq. (40) corresponds to the leading term of Eq. (35), to which the anomalous magnetic moments provide additional corrections. Using the converged Dirac wave-functions with exponential finite-Coulomb and finite vacuum polarization potentials (rather than Schrödinger wave-functions) we calculate the expectation value of r^{-3} and find

$$\Delta E_{\rm HFS}^{2{\rm P}_{1/2}} = 7.62042 \text{ meV}. \tag{41}$$

The addition of the (point) vacuum polarization potential to the point-Coulomb potential increases the splitting by 0.0017(5) meV, and the introduction of the finite-Coulomb potential increases this further by 0.0045(5) meV to arrive at the value above.

C. $2{\rm P}_{3/2}$ Hyperfine Structure

Following the same method as the previous subsection, we can similarly calculate the energy levels for the $2{\rm P}_{3/2}^{F=1}$ and $2{\rm P}_{3/2}^{F=2}$ eigenstates. The $2{\rm P}_{3/2}$ hyperfine structure as derived in Ref. [4] is given by

$$\Delta E_{HFS}^{2{\rm P}_{3/2}} = E_F\left[\frac{2}{15} - \frac{a_\mu}{30} + \frac{m_\mu(1+2\kappa)}{12m_p(1+\kappa)}\right], \tag{42}$$

where E_F is given in Eq. (36). Alternatively, inserting the relevant values for this state into Eq. (38) and using the converged Dirac wave-functions we find

$$\Delta E_{\rm HFS}^{2{\rm P}_{3/2}} = 3.04151 \text{ meV} \tag{43}$$

when the potential consists of the exponential finite-Coulomb and point vacuum polarization potentials. For this state, the addition of the (point) vacuum polarization potential to the point-Coulomb potential increases the splitting by 0.0007(5) meV to the value above, and the introduction of the finite-Coulomb potential was found to have no effect within the limits of our calculation, so too was the introduction of the finite vacuum polarization potential.

IX. SUMMARY

In the summary tables to follow we refer to various iterations of our calculations in which we calculate the wave-function in the presence of point-Coulomb (C); finite-Coulomb (FC); point vacuum polarization (VP); and finite vacuum polarization (FVP) potentials. The dependences on $\langle r_p^n\rangle$ are extracted by fitting energy shifts calculated at various values of r_p to a cubic of the form given in Eq. (17) for the case of a Coulomb-only potential, and with the addition of a term proportional to 1 when including the vacuum polarization (to account for the 2S–2P splitting). We note that the calculations for the $2{\rm P}_{1/2}$ eigenstate are of no relevance to the measured transition, but are of value for comparison to other studies. We also note the lack here of the energy shift attributed to a mixing between the $2{\rm P}_{1/2}$ and $2{\rm P}_{3/2}$ $F = 1$ states, as discussed in Ref. [10] for comparison to Ref. [1] where it is also absent.

TABLE I: Contributions to the 2S–2P Lamb shift with comparison to values found in Pohl *et al.* [1]. Values are all in meV. Errors in the Dirac calculations are taken to be 0.5 μeV as per Section IV. The listed corrections are already included in our Dirac calculations. All further corrections to both the perturbative calculation and our calculation are contained in 'Remaining Corrections'.

Contribution	Pohl *et al.*	Carroll *et al.*
Dirac ($V = V_{\rm C} + V_{\rm VP}$)		205.1706
Dirac ($V = V_{\rm FC}$)		-5.2000 $\langle r_p^2 \rangle$ + 0.0350 $\langle r_p^3 \rangle$
Dirac ($V = V_{\rm FC} + V_{\rm VP}$)		205.171 - 5.2169 $\langle r_p^2 \rangle$ + 0.0353 $\langle r_p^3 \rangle$
Dirac ($V = V_{\rm FC} + V_{\rm FVP}$)		205.182 - 5.2519 $\langle r_p^2 \rangle$ + 0.0546 $\langle r_p^3 \rangle$
Relativistic one loop VP	205.0282	
Polarization insertion in two Coulomb lines	0.1509	
Finite size effects	-5.2262 $\langle r_p^2 \rangle$ + 0.0347 $\langle r_p^3 \rangle$	
Subtotal:	205.179 - 5.2262 $\langle r_p^2 \rangle$ + 0.0347 $\langle r_p^3 \rangle$	205.182 - 5.2519 $\langle r_p^2 \rangle$ + 0.0546 $\langle r_p^3 \rangle$
Remaining Corrections	0.878	
Total:	206.057 - 5.2262 $\langle r_p^2 \rangle$ + 0.0347 $\langle r_p^3 \rangle$	206.060 - 5.2519 $\langle r_p^2 \rangle$ + 0.0546 $\langle r_p^3 \rangle$

TABLE II: Contributions to the $2S_{1/2}$ hyperfine splitting with comparison to values found in Martynenko [5]. Values are all in meV. Errors in the Dirac calculations are taken to be 0.5 μeV as per Section IV. The listed corrections are already included in our Dirac calculations. All further corrections to both the perturbative calculation and our calculation are contained in 'Remaining Corrections'. We note that the 'Proton structure corrections of order α^5' does not include considerations of finite-size in the XXXXX, though we have not calculated the correct value here.

Contribution	Martynenko	Carroll *et al.*
Dirac ($V = V_{\rm C}$)		22.8229
Dirac ($V = V_{\rm FC}$)		22.6960
Dirac ($V = V_{\rm C} + V_{\rm VP}$)		22.8976
Dirac ($V = V_{\rm FC} + V_{\rm VP}$)		22.7702
Dirac ($V = V_{\rm FC} + V_{\rm FVP}$)		22.7690
Fermi Energy E_F	22.8054	
Relativistic correction $\frac{17}{8}(Z\alpha)^2 E_F$	0.0026	
VP corrections of orders α^5, α^6 in the second order of perturbation series	0.0746	
Proton structure corrections of order α^5	-0.1518	
Proton structure corrections of order α^6	-0.0017	
Subtotal:	22.7291	22.7690
Remaining Corrections	0.0857	
Total:	22.8148	22.8547

TABLE III: Contributions to the $2P_{1/2}$ hyperfine splitting with comparison to values found in Martynenko [4]. Values are all in meV. Errors in the Dirac calculations are taken to be 0.5 μeV as per Section IV. The listed corrections are already included in our Dirac calculations. All further corrections to both the perturbative calculation and our calculation are contained in 'Remaining Corrections'. The leading term and contribution from the proton magnetic moment (included in 'Remaining Corrections' here, but included at order α^4 in the reference) have been extracted from calculations of Martynenko. We note the minor error in the summary contribution of Ref. [4] for this state, perhaps arising from round-off error. here.

Contribution	Martynenko	Carroll *et al.*
Dirac ($V = V_{\rm C}$)		7.6141
Dirac ($V = V_{\rm C} + V_{\rm VP}$)		7.6159
Dirac ($V = V_{\rm FC} + V_{\rm VP}$)		7.6204
Dirac ($V = V_{\rm FC} + V_{\rm FVP}$)		7.6204
Leading contribution	7.6018	
Relativistic correction	0.0011	
Subtotal	7.6029	7.6204
Remaining Corrections	362.6293	
Total:	7.9644	7.9830

TABLE IV: Contributions to the $2P_{3/2}$ hyperfine splitting with comparison to values found in Martynenko [4]. Values are all in meV. Errors in the Dirac calculations are taken to be 0.5 μeV as per Section IV. The listed corrections are already included in our Dirac calculations. All further corrections to both the perturbative calculation and our calculation are contained in 'Remaining Corrections'. The leading term and contribution from the proton magnetic moment (included in 'Remaining Corrections' here, but included at order α^4 in the reference) have been extracted from calculations of Martynenko.

Contribution	Martynenko	Carroll *et al.*
Dirac ($V = V_{\rm C}$)		3.0408
Dirac ($V = V_{\rm C} + V_{\rm VP}$)		3.0415
Dirac ($V = V_{\rm FC} + V_{\rm VP}$)		3.0415
Dirac ($V = V_{\rm FC} + V_{\rm FVP}$)		3.0415
Leading contribution	3.0407	
Relativistic correction	0.0001	
Subtotal	3.0408	3.0415
Remaining Corrections	0.3519	
Total:	3.3926	3.3934

X. CONCLUSIONS

After careful consideration of the various contributions to the measured transition energy of Pohl *et al.* [1], calculated consistently using the Dirac equation with appropriate potentials, and following the addition of the required corrections to these calculations (taking further care to avoid overcounting issues), we find no single term contains a discrepancy with the perturbative results of sufficient magnitude to account for the difference between theory and experiment here. These calculations nonetheless provide a useful insight into the reliability of the perturbative calculations, and allow a simpler approach to future investigations.

While it remains possible that one or more of the higher-order corrections to the terms calculated in this work contain errors of a suitable magnitude to affect the analysis of Ref. [1], the precision to which the Dirac and perturbative calculations agree for the terms calculated here would suggest that this will not be the case.

We further note that our calculations of a hitherto overlooked contribution arising from off-mass-shell effects for the proton (which are negligible for electronic hydrogen) provide a natural solution to the proton radius problem [11], and as such the combination of these two sets of calculations may provide a complete description of the measured transition in muonic hydrogen with no discrepancy in the rms charge radius of the proton. Due to the uncertain magnitude of

TABLE V: Contributions to the 2P fine-structure splitting with comparison to values found in Borie *et al.* [3]. Values are all in meV. Errors in the Dirac calculations are taken to be 0.5 μeV as per Section IV. The listed corrections are already included in our Dirac calculations. All further corrections to both the perturbative calculation and our calculation are contained in 'Remaining Corrections'. The finite vacuum polarization potential is considered to lead to a very small perturbation for P states, and as such is neglected here.

Contribution	Borie *et al.*	Carroll *et al.*
Dirac ($V = V_{\rm C}$)	8.4156	8.4156
Dirac ($V = V_{\rm FC}$)		8.4156
Dirac ($V = V_{\rm C} + V_{\rm VP}$)		8.4206
Dirac ($V = V_{\rm FC} + V_{\rm VP}$)		8.4206
Dirac ($V = V_{\rm FC} + V_{\rm FVP}$)		8.4206
Uehling (VP)	0.0050	
Subtotal	8.4206	8.4206
Remaining Corrections	0.06852	
Total:	8.3521	8.3521

TABLE VI: Sum of contributions to the measured experimental transition energy shown in Fig. 1. Values are all in meV. The individual perturbative contributions (Various *et al.*) are taken from the previous tables. In each case, the value given for the Dirac calculation is calculated using the combination of finite-Coulomb and finite vacuum polarization potentials ($V = V_{\rm FC} + V_{\rm FVP}$). The fractional factors for the hyperfine splittings are inserted for relevance to the measured transition, and are calculated via angular-momentum splitting rules.

Contribution	Various *et al.*	Carroll *et al.*
$2S_{1/2}$-$2P_{1/2}$ Lamb shift (constant)	206.057	206.060
$2S_{1/2}$-$2P_{1/2}$ Lamb shift (finite-size)	-5.2262 $\langle r_p^2 \rangle$ + 0.0347 $\langle r_p^3 \rangle$	-5.2519 $\langle r_p^2 \rangle$ + 0.0546 $\langle r_p^3 \rangle$
$2P_{1/2}$ Fine Structure	8.3521	8.3521
$\frac{1}{4} \times 2S_{1/2}$ Hyperfine	−5.7037	−5.7137
$\frac{3}{8} \times 2P_{3/2}$ Hyperfine	1.2722	1.2725
Various *et al.* Total (Perturbative)	**209.9779 - 5.2262 $\langle \mathbf{r_p^2} \rangle$ + 0.0347 $\langle \mathbf{r_p^3} \rangle$**	
Carroll *et al.* Total (Dirac)	**209.9709 - 5.2519 $\langle \mathbf{r_p^2} \rangle$ + 0.0546 $\langle \mathbf{r_p^3} \rangle$**	

this effect, it is incorrect to complete the analysis of this transition to predict a proton rms charge radius—we await the results of current and future experiments which will be ascertain the strength of this contribution, after which the analysis will be sensible.

Nonetheless, we note that our calculations predict that the transition energy for the $2P_{3/2}^{F=2}$ to $2S_{1/2}^{F=1}$ transition in muonic hydrogen is smaller in magnitude than that which is predicted by the perturbative calculations, and that analysis of this data under the assumption that no further terms are required leads to the following values for the proton rms charge radius when fit to the experimental data;

$$\textbf{Pohl } et\ al.: \quad \langle r_p \rangle = 0.841831(67)\ \text{fm},$$

$$\textbf{Carroll } et\ al.: \quad \langle r_p \rangle = 0.840301(5)\ \text{fm}.$$

The value of Pohl *et al.* is taken as the solution to the cubic equation

$$209.9779 - 5.2262 \langle r_p^2 \rangle + 0.0347 \langle r_p^3 \rangle = 206.2949, \tag{44}$$

where the last term corresponds to the quoted value of the measured transition in Ref. [1]. This extracted $\langle r_p \rangle$ differs from the central value quoted in [1]; 0.84184(67), though the difference is within the quoted errors. The value of Carroll *et al.* is extracted in the same manner, with the left-hand-side of Eq. (44) taken from the relevant conclusion line of Table (VI).

Acknowledgments

This research was supported in part by the United States Department of Energy (under which Jefferson Science Associates, LLC, operates Jefferson Lab) via contract DE-AC05-06OR23177 (JDC, AWT); grant FG02-97ER41014 (GAM); and grant DE-FG02-04ER41318 (JR), and by the Australian Research Council and the University of Adelaide (JDC, AWT). GAM and JR gratefully acknowledge the support and hospitality of the University of Adelaide while the project was undertaken.

---

[1] R. Pohl, A. Antognini, F. Nez, F. D. Amaro, F. Biraben, et al., Nature **466**, 213 (2010).
[2] P. J. Mohr, B. N. Taylor, and D. B. Newell, Rev. Mod. Phys. **80**, 633 (2008), 0801.0028.
[3] E. Borie, Phys.Rev. **A71**, 032508 (2008), physics/0410051.
[4] A. Martynenko, Phys.Atom.Nucl. **71**, 125 (2008), hep-ph/0610226.
[5] A. Martynenko, Phys.Rev. **A71**, 022506 (2005), hep-ph/0409107.
[6] J. Rafelski, Phys. Rev. **D16**, 1890 (1977).
[7] J. Carroll (2010), nucl-th/xxxxxx.
[8] B. Fricke, Z. Phys. **218**, 495 (1969).
[9] M. Weissbluth, *Atoms and molecules* (Academic Press, 1978), ISBN 9780127444505.
[10] K. Pachucki, Phys.Rev. **A53**, 2092 (1996).
[11] G. A. Miller, A. W. Thomas, J. D. Carroll, and J. Rafelski (2011), * Temporary entry *, arXiv:1010.3421.